Characterizing electronic structure motifs in β-UH_3

Christopher D. Taylor
Materials Science and Technology Division, Mail stop G755, Los Alamos National Laboratory, Los Alamos, New Mexico 87545, USA

(Received 23 August 2010; published 7 December 2010)

Density-functional theory was used to evaluate the electronic structure of β-UH_3 over a range of unit-cell volumes. Using population analysis methods (projection and topological) the magnetic and electronic structure were probed. It was found that the topological analysis led to the description of the β-UH_3 crystal as partially ionic, with delocalization of electrons running across the U-U bonds that form one-dimensional chains in the (100), (010), and (001) directions. Magnetic moments were divided into delocalized (itinerant) moments running along the chains of the crystal, and localized moments, for the U atoms sited at the bcc sites. The experimental observation regarding the identical magnetic properties for the two distinct sites was shown to result from a coincidence in the moments and electronic configurations of the uranium atoms obtained at the equilibrium volume whereas these properties diverged at higher and lower cell volumes. The electronic structure was interpreted in terms of three primary categories of orbital overlap: U-U of the dissimilar sites, U-U of the chain sites, and U-H effects, each having separate volume dependencies. Analysis of the magnetovolumetric properties of α-UH_3, in which U-U bonding at the chain sites does not occur, shows features that support this analysis.

DOI: 10.1103/PhysRevB.82.224408 PACS number(s): 75.10.Lp, 71.15.Mb

I. INTRODUCTION

Uranium hydride (UH_3) is known to form in two separate crystal structures, both members of the space group 223 (Cr_3Si).[1,2] The two allotropes are distinguished by the positions of the atoms: in the α phase the U atoms assume the Si positions in the Cr_3Si structure, with the hydrogen atoms adopting the Cr positions; in the β phase the U atoms assume both the Cr and Si positions, with the H atoms occupying tetrahedral interstitials in the structure (see β phase in Fig. 1). The volumes of the two phases are relatively similar, with the α phase being slightly smaller. The α phase is metastable, and hence the β phase has been the more widely studied.[3,4]

β-UH_3 is magnetic and the two symmetrically inequivalent U atoms appear to be magnetically equivalent.[5] The electronic configuration of the U atoms is not well understood, particularly regarding the question of itinerant versus localized magnetic properties, or the nature of bonding being covalent or ionic in nature. Although Ward *et al.* proposed a combination of localization and itinerancy, for example, Andreev *et al.* have more recently proposed that the magnetic moment is predominantly itinerant.[6,7] Even more recently, it has been suggested by Gouder *et al.* that the magnetic moments are only weakly itinerant, and may localize following photoemission.[8] Such questions are an instance of the more general topic of charge transfer and correlation sensitivity for partially ionic materials and the actinide elements.

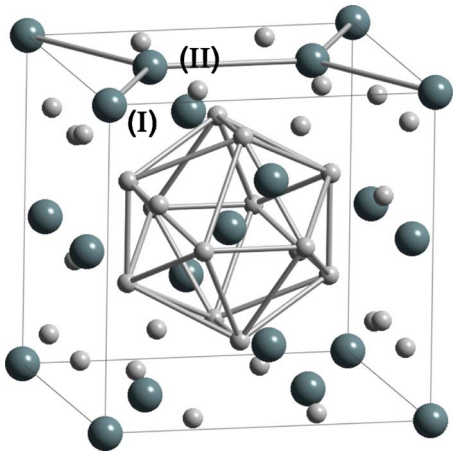

FIG. 1. (Color online) β-UH_3 with U positions (I) the bcc sites and (II) the chain sites marked.

In the β phase of UH_3, two U atoms are in relatively close proximity (in the Cr positions) and it is possible that there is some itinerancy in the magnetism via these one-dimensional U chains. Such an effect would depend on the extent of overlap between the valence d and f orbitals of the atoms, and could therefore vary significantly with small changes in volume; similar to the complex properties observed for Pu metal.[9] On the other hand, the α phase has the H atoms on the Cr sites and the U atoms on the Si sites only, thus we may expect differences in the electronic structure to emerge, especially when studying the effect of volume changes upon the magnetic moment.

Herein we utilize density-functional theory to compute the electronic structure for β-UH_3 and analyze the resulting charge and orbital distributions to provide insights into the magnetic and bonding properties of this material. It will be shown that the nature of bonding varies significantly with small changes in the unit-cell volume, particularly regarding the overlap of f electrons, and that this subtle effect leads to an overprediction of the magnetic properties of the hydride in the density-functional treatment. Furthermore, analysis of the magnetic properties of α-UH_3 will be shown to support the interpretation of electronic structure effects in the β phase, by comparison of the magnetovolumetric structure and consideration of the crystallographic differences between the two phases.

II. COMPUTATIONAL METHOD

The electronic structure problems related to the determination of the magnetic and charge properties described herein were solved using the Vienna *ab initio* simulation package (VASP).[10] The projector augmented wave (PAW) functions for uranium and hydrogen supplied with version 4.6 of VASP were used without modification. The PW91 exchange-correlation functional was also adopted.[11] Unlike standard density-functional theory calculations of UO_2,[12] generalized-gradient calculations of UH_3 have been shown to reproduce the band structure and lattice constant in good agreement with experiment.[8,15] UH_3 is known to be metallic,[8] and hence standard density-functional theory treatments are expected to give a good description of the electronic structure, which is not always the case for band-gap materials, such as UO_2.[12]

Tests of the energy convergence with respect to the k-point mesh size and energy cutoff lead to the choice of an energy cutoff of 500 eV and a gamma-centered Monkhorst-Pack k-point mesh generated using a generating length of 40 Å.[13] This choice of k-point mesh corresponds to a $10\times10\times10$ mesh and a $6\times6\times6$ mesh for the α-UH_3 and the β-UH_3 unit cells, respectively. The resulting energies were converged with respect to energy cutoff and k-point mesh to within 2 meV (0.15 mRy). To perform relaxations the Methfessel-Paxton smearing method[14] was used to provide more accurate forces (width of 0.2 eV), whereas for single-point calculations the Bloechl tetrahedron method was adopted.[15] Self-consistent electronic-structure calculations were iterated to within 0.1 meV, and, for geometric relaxations, iterations over the lattice positions were performed until forces were less than 0.05 eV/Å. The relaxations were performed using the conjugate gradient method. Scalar-relativistic calculations were performed for all systems in which case the PAW-core contribution is considered to supply all of the relativistic contribution to the electronic structure. Previous work showed that explicit inclusion of the spin-orbit coupling between electronic quantum numbers did not affect the magnetic or electronic properties of the hydride.[16,17] Furthermore, a zero orbital moment has calculated for the uranium atoms in this compound.

Electronic-structure properties were obtained by applying Bader's topological charge analysis coded by Henkelman and co-workers.[18] Topological analysis deconstructs the charge density into atomic components, based on topological features of the charge density, such as the Laplacian.[19] Using this technique it is possible to examine the bonding arrangements between atoms and the partial charges on each atom. Complementary to this technique are the projected density of states plots calculated by VASP based on arbitrary atomic radii assigned to each atom type and projections of the atomic-orbital-like spherical harmonics centered at the atom sites.

III. RESULTS AND DISCUSSION

A. Topological decomposition of the atomic volumes

The nominal charge (oxidation state) on uranium in UH_3 is +3.[20] A reduction in charge would imply a mixing between covalent and ionic interactions in the U-H bonds. The charge on U in sites I and II were determined using Bader's method of topological charge-density partitioning,[18,19] in which dividing surfaces are constructed between atoms based on gradients and second derivatives of the charge-density map obtained from first-principles computations. The resulting charges, plotted as a function of the volume of the UH_3 cell, are shown in Fig. 2.

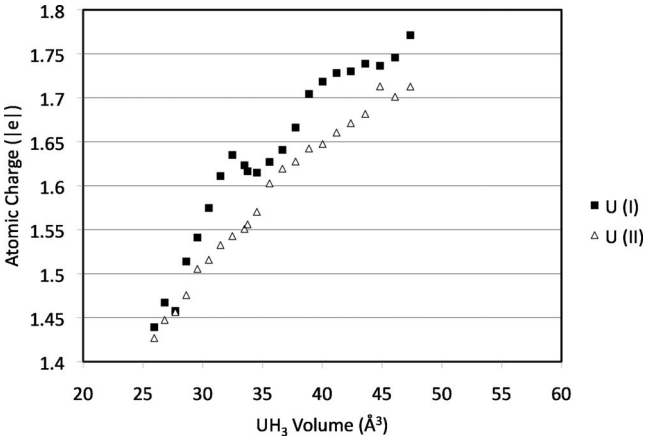

FIG. 2. Atomic charge on uranium plotted against the volume of the UH_3 unit cell for U sites (I) and (II), see Fig. 1.

At the theoretical equilibrium volume (35.6 $Å^3$) the charges on U at sites I and II are close to equal, at a value of $1.6|e|$, where $|e|$ indicates the magnitude of the charge of an electron. This value indicates that there is significant covalent mixing between U and H in the UH_3 crystal. Overall the charge on U at site (II) is lower than the charge on U at site (I). Site (II) corresponds to the chained sites in the UH_3 lattice, which we shall show later have some additional covalent mixing between the neighboring site (II). This effect may lead to additional reduction in the polarization of the U atoms at these sites.

There is a local maximum in the charge on U at site (I) just below the equilibrium volume, and just above the equilibrium volume the charge steeply increases. The reduction in covalency due to expanding bond lengths (and hence orbital overlap) between U and H explains the increase in ionicity with an increase in volume, but it does not explain the local maximum that occurs just below this point.

Topological analysis of the atomic volumes also reveals information regarding the U-U bonding in the site (II) positions. Inspection of Fig. 1 indicates that the U-U bond lengths in these sites are lower than those between the (I) sites, or the distances between the (I) and (II) positions. Furthermore, the atoms in the (II) sites form linear chains running throughout the entire crystal. At the equilibrium volume the U-U distance is below the Hill limit for delocalized magnetism,[21] and hence, it is possible that some itinerant magnetic behavior may result from this geometry. We have performed a topological decomposition of the atomic volumes, and plotted the volumes in Fig. 3.

The topological decomposition indicates that the U(II) atoms share an interfacial atomic plane, indicating that there is direct bonding between the two metal atoms. On the other

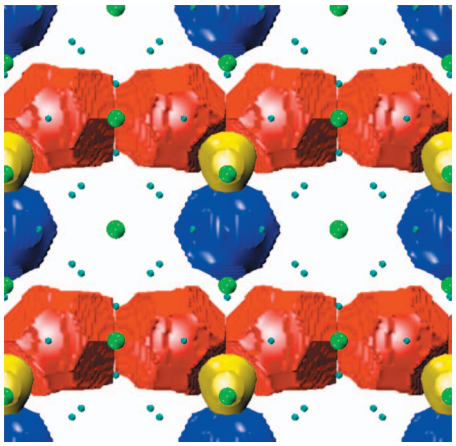

FIG. 3. (Color) Atomic volumes for selected U(I) rendered in blue, U(II) rendered in red, and H rendered in yellow. H atoms without volumes are rendered as white spheres, and the uranium atoms as green spheres.

hand, the U atoms at site (I) do not share an interfacial plane with any other U atoms, and hence bonding for these atoms is restricted to U-H as shown about the rendered H atomic volume in Fig. 3. Topological analysis of the spin density in Fig. 4 corroborates this interpretation and shows that the spin on the uranium atoms is divided into a localized part on site (I) and a delocalized or itinerant part on site (II).

The magnetic moments can be directly calculated through either topological analysis or by projecting atomic orbitals onto the charge density within some radial cutoff of the nuclear positions. The atomic charges as well as the individual and total magnetic moments, computed by both methods, are tabulated in Table I for U(I), U(II), and H. It can be seen that, whereas the charges are very sensitive to the method used (as is typical in charge population analysis), the magnetic moments are similar, with the topological moments being larger. Larger topological moments are consistent with smaller topological charges, in that more of the electron density is apparently being captured via the topological decomposition of the charge density, compared to the spherical projections used in the radial cut-off method. In addition, the topological charges add up to zero due to the complete partitioning of the electron density whereas 3.45 electrons are absent from the counting scheme used in projection. The topological scheme would indicate that the hydrogen atoms are partially anionic (–0.53 charge), which is consistent with a partial ionicity, whereas the projection method would indicate that the substance is more metallic in nature, with a significant delocalization of both the H and U electrons (an embedded proton model). Both methods indicate slightly higher magnetic moments for the U atoms in the (II) site.

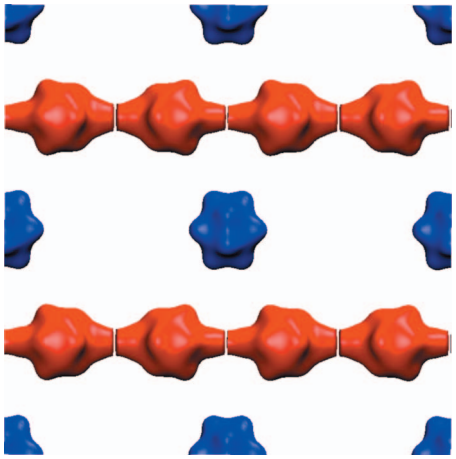

FIG. 4. (Color) Topological decomposition of the spin density on uranium atoms. The *f*-orbital shape of the spin density is apparent. Breaks in the contours at the interfacial planes connecting cells are an artifact of the plotting procedure.

TABLE I. Charges and magnetic moments obtained from radial projection and topological (Bader) decomposition.

	Q_{proj}	μ_{proj}	Q_{Bader}	μ_{Bader}
U(I)	+2.10	2.21	1.63	2.43
U(II)	+2.17	2.38	1.60	2.64
H	+0.431	0	–0.53	0
Totals	+3.45	2.34	0	2.59

The moments determined from theory are higher than the moments obtained experimentally (NMR and neutron diffraction give a moment around 1.5 μ_B, and field measurements give around 1.0 μ_B).[20,22,23] In order to examine why this might be the case we also plot the variation in the total magnetic moment, as well as the projected moment, with variation in the cell volume. These plots are shown in Figs. 5 and 6, respectively.

At the equilibrium volume of 35.6 Å the system magnetization is at a sensitive point at which the gradient of the magnetic moment with respect to the system volume is large. Thus subtle fluctuations in the cell volume, can lead to large changes in the predicted magnetic moment. Increasing the volume slightly could lead to moments near the higher shoulder value of 2.8 μ_B per UH_3 formula unit. Slightly decreasing the volume would lead to moments at the lower shoulder

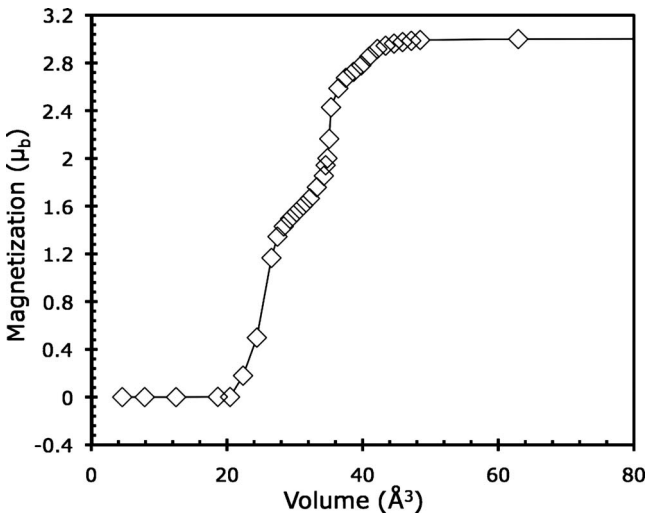

FIG. 5. UH_3 magnetization plotted against the volume of the unit cell.

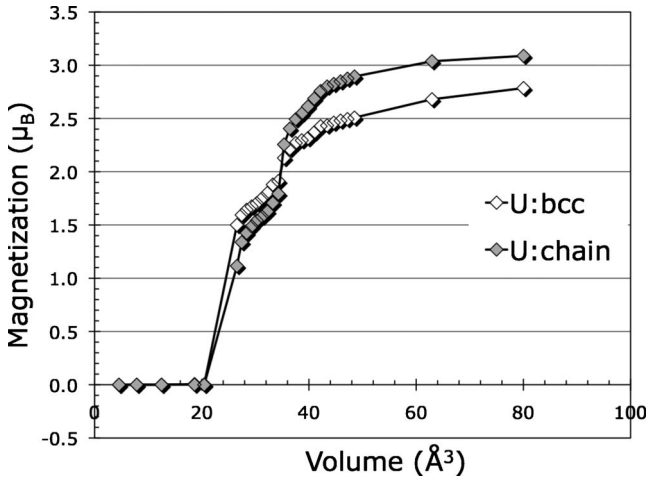

FIG. 6. Projected UH_3 magnetization [U(I)=bcc, U(II)=chain] plotted against the volume of the unit cell.

edge of around 1.5–1.6 Å. As observed by Andreev, the U-U distances in UH_3 are close to the Hill limit, and thus large fluctuations in the localization of f electrons are expected with volume at this point.[6] Small errors in the volumes and/or extent of electron overlap therefore arising from the approximations made in the mean field density-functional approach, therefore, could lead to significant departures from the expected magnetic moment. Such appears to be the case here. Examination using spin-orbit coupling showed that there was no orbital quenching of the moment, that could potentially bring the theoretical value in line with the experimental moments.

The appearance of multiple shoulders in the moments, as shown in Fig. 5, is reflective of the variety of bonding opportunities in the UH_3 crystal. To understand this more completely, we turn to the analysis of the projected moments as shown in Fig. 6.

The bonding opportunities present in the UH_3 crystal can be broken down into three chief categories of significance: U-H, U(II)-U(II), and U(I)-U(II). As a function of volume one may expect, based on the particular lattice geometries, that U-H bonding will appear first upon compression of the expanded crystal, followed by U(II)-U(II) bonding via the chains running along the cubic planes, and finally U(I)-U(II) interactions as the crystal is further compressed. Thus it would be expected that the magnetization plot would show three main thresholds as the orbital overlap boundaries are crossed. Examination of the data shows that this is indeed the case. Above a volume of 50 Å^3 the magnetization of both atoms is close to 3, corresponding to the ionic U(+3) state with $7s^05f^3$ state. Diminishing the volume leads to small continuous changes in the magnetization, and then at 42 Å^3 both U(I) and U(II) show a step decrease in the magnetization, presumably due to the development of the partial covalent interactions with H. At around 36–38 Å^3 the U(II) atoms show a significant drop in magnetization, and this corresponds to the entrance into the Hill limit for f-f overlap for these atoms.[21] There is a smaller step decrease in magnetization for the U(I) atoms at this point also, which we attribute to a secondary affect. It is also possible that there is overlap between the various transition points proposed herein that add additional complexity to the structure of the curves. Between 36 and 25 Å^3 the magnetization holds fairly level at 1.5–1.8 μ_B, and then at 25 Å^3 there is a complete loss of magnetization as orbital overlap between U(I) and U(II), as well as H, becomes overwhelming. The density of states plots in Fig. 7 corroborate this interpretation of increase localization toward metallization with decreasing volume. Parenthetically, the density of states calculated for UH_3 at the equilibrium volume (around 36 Å^3) is consistent with the UPS valence-band spectra reported by Gouder, in that there is a band from 1 eV to the Fermi level, and a broad band from 8 to 3 eV.[8] It is also noteworthy that the U(I) and U(II) atoms follow different magnetization curves, yet at the equilibrium volume, the magnetic moments coincide with one another, which is in agreement with the experimental results.[5]

It is helpful to consider the extent of d-f hybridization occurring in these compounds. It was noted above that at expanded volumes, U is expected to tend to U^{+3} with a $7s^05f^3$ configuration. Analysis of the projected occupation numbers for the uranium atoms indicates that d mixing occurs in a continuous, exponentially increasing fashion as the volume shrinks. This feature is consistent with both U(I) and U(II) atoms. Notably, it is at the equilibrium volume that f occupation reaches a minimum and then begins to increase again as the f-f overlap improves with larger increases in volume. For U(II) this minimum occurs at a slightly more reduced volume. At volumes larger than this point, d occupation is achieved by donation from the f orbitals. At volumes smaller than this point, it apparently arises due to overlap effects. Change in f overlap with compression is relatively flat until the volume of 25 Å^3 is reached, which coincides with the onset of metallization in the magnetization data. The differences in the f-occupation plots for U(I) and U(II) are a consequence of the differing geometric placements of these two atoms, in that more f-f overlap is achievable for U(II) atoms as a consequence of their closer range of interaction, unimpeded by interference from H atoms (Fig. 8).

Population analysis at the equilibrium volume indicates that a $7s^26p^66d^15f^3$ configuration is pertinent, which is an approximate +2 charge state, as indicated by both topological (on the lower side: $1.6|e|$) and projected ($2.1|e|-2.2|e|$) techniques. The electron configurations are more or less identical between the two U sites.

B. Comparison of α-UH_3 and β-UH_3 magnetovolumetric response

The metastable phase of UH_3, known as α-UH_3, bears crystallographic similarity to the β phase but has the H atoms sitting in the "chain" positions of the Cr_3Si crystal structure. This positioning prevents the direct U-U bonding that is manifested in the β phase. As a result, the magnetovolumetric curve for the α phase has less structure, as there is only one unique site for the U atom (the bcc position) and therefore only one kind of U-U interaction possible upon compression. Figure 9 displays the dependence of the magnetic

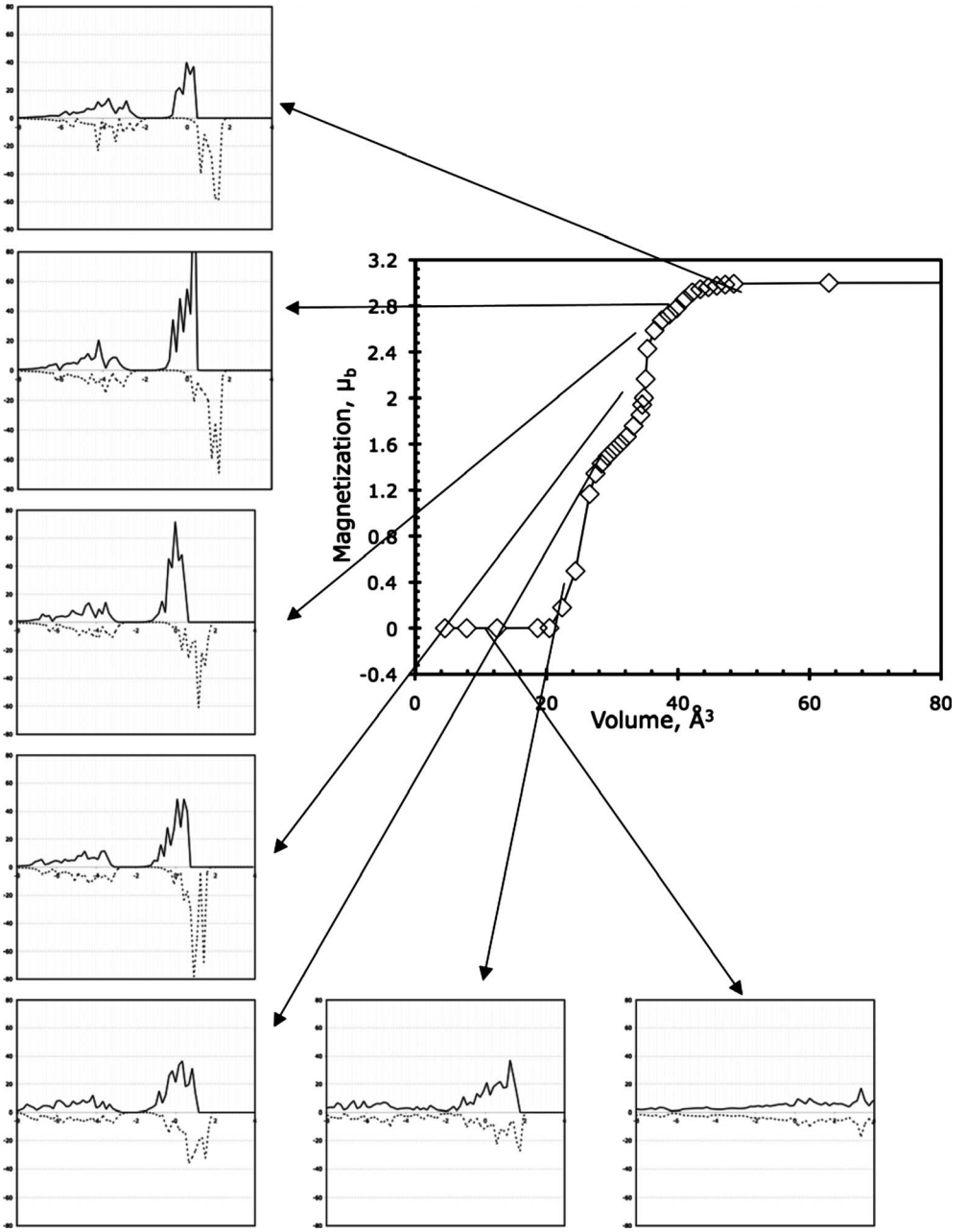

FIG. 7. DOS plots showing progressive loss of magnetization as a function of volume.

moment of U upon the unit volume for both α and β phases over the range of 15 to 45 Å^3. It can be seen from this figure that, upon compression the magnetic moment of the α phase is slower to quench, presumably due to the absence of the one-dimensional U-U interactions which help to quench the magnetism in the β phase (by coupling the unpaired electrons on the uranium atoms and thereby reducing the localized moment, yet at the same time allowing an itinerant moment to emerge). At the equilibrium volume of 35 Å the magnetic moment of U exceeds that in the β phase, and is close to the isolated U atom moment of 3 μ_B. Again this may be attributed to the greater U-U distances present in the α phase.

IV. SUMMARY AND CONCLUSIONS

By performing electronic-structure calculations on UH_3 followed by population analysis via the projection and topological methods, insights have been gained into the nature of the electronic structure in this material. Topological analysis indicates that the U metal atoms are not completely oxidized to U^{+3} but have some covalency due to both U-H interactions, as well as direct U-U binding at the chain sites (I). In addition both localized and itinerant magnetism is apparent, leading to unique behaviors for the U(I) and U(II) sites. Despite the uniqueness of the two sites, their measurable properties (moment, electron configuration) coincide at the equilibrium volume. Density-functional theory appears to

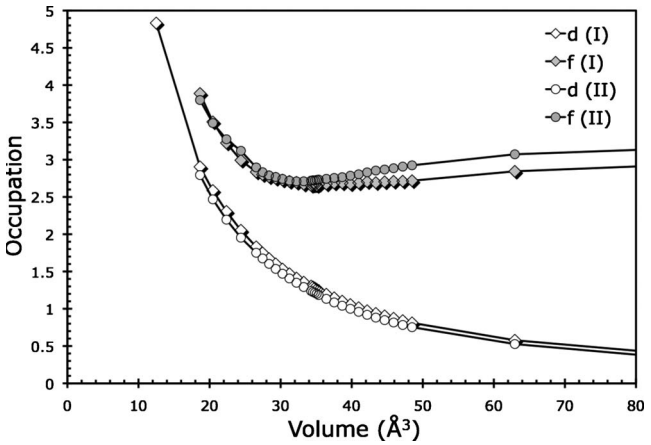

FIG. 8. *d-f* hybridization in uranium atoms as a function of the UH_3 unit volume.

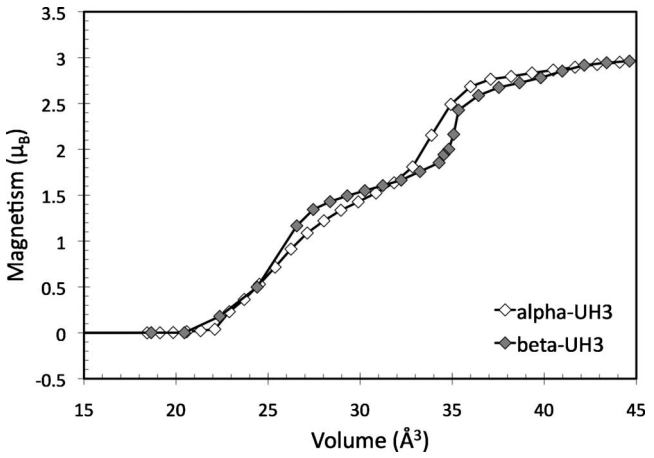

FIG. 9. Magnetic moment response of uranium hydride to changes in the unit volume for α and β phases.

overestimate the magnetic moment of the metal ions at equilibrium, and this is attributed to the severity of the gradient of magnetic properties with respect to small changes in volume about the equilibrium point.

The volume-dependent changes in magnetic and charge properties are attributed to the stepwise introduction of distinct bonding effects upon compression of the expanded crystal: the appearance of U-H binding, the development of U-U *f*-orbital overlap at the chain sites, and finally, complete metallization of all U atoms upon severe compression.

Population analysis leads to different predictions of behavior depending upon the method used: projection analysis suggests that the UH_3 crystal is completely metallic, however, many electrons are absent from the full electron count using this method; the complete accounting method of topological analysis leads to a partially ionic crystal description, in which hydrogen is partially anionic. In addition to being more appealing due to the lack of arbitrary radial cut-off points, this latter description also appears more consistent with the band-structure analysis, that shows that full metallization does not occur until higher levels of lattice compression are reached.

ACKNOWLEDGMENTS

The author gratefully acknowledges helpful discussions with R. S. Lillard, J. L. Smith, and R. K. Schulze at Los Alamos National Laboratory. We also acknowledge the Enhanced Surveillance Program (Tom Zocco) at Los Alamos National Laboratory for funding this work. The Los Alamos National Laboratory is operated by Los Alamos National Security LLC for the National Nuclear Security Administration of the U.S. Department of Energy under Contract No. DE-AC52-06NA25396.

[1] R. E. Rundle, J. Am. Chem. Soc. **73**, 4172 (1951).
[2] R. N. R. Mulford, F. H. Ellinger, and W. H. Zachariasen, J. Am. Chem. Soc. **76**, 297 (1954).
[3] F. D. Manchester and A. San-Martin, J. Phase Equilib. **16**, 263 (1995).
[4] J. B. Condon, J. Phys. Chem. **79**, 42 (1975).
[5] W. Bartscher, A. Boeuf, R. Caciuffo, J. M. Fournier, W. F. Kuhs, J. Rebizant, and F. Rustichelli, Solid State Commun. **53**, 423 (1985).
[6] A. V. Andreev, S. M. Zadvorkin, M. I. Bartashevich, T. Goto, J. Kamarad, Z. Arnold, and H. Drulis, J. Alloys Compd. **267**, 32 (1998).
[7] J. W. Ward, L. E. Cox, J. L. Smith, G. R. Stewart, and J. H. Wood, J. Phys. Colloq. **40**, C4 (1979).
[8] T. Gouder, R. Eloirdi, F. Wastin, E. Colineau, J. Rebizant, D. Kolberg, and F. Huber, Phys. Rev. B **70**, 235108 (2004).
[9] P. Söderlind and B. Sadigh, Phys. Rev. Lett. **92**, 185702 (2004).
[10] G. Kresse and J. Furthmüller, Phys. Rev. B **54**, 11169 (1996).
[11] J. P. Perdew, J. A. Chevary, S. H. Vosko, K. A. Jackson, M. R. Pederson, D. J. Singh, and C. Fiolhais, Phys. Rev. B **46**, 6671 (1992).
[12] S. L. Dudarev, D. N. Manh, and A. P. Sutton, Philos. Mag. B **75**, 613 (1997).
[13] H. J. Monkhorst and J. D. Pack, Phys. Rev. B **13**, 5188 (1976).
[14] M. Methfessel and A. T. Paxton, Phys. Rev. B **40**, 3616 (1989).
[15] P. E. Blöchl, O. Jepsen, and O. K. Andersen, Phys. Rev. B **49**, 16223 (1994).
[16] C. D. Taylor, T. Lookman, and R. S. Lillard, Acta Mater. **57**, 4707 (2009).
[17] C. D. Taylor and R. S. Lillard, Acta Mater. **58**, 1045 (2010).
[18] G. Henkelman, A. Arnaldsson, and H. Jónsson, Comput. Mater. Sci. **36**, 354 (2006).
[19] R. Bader, *Atoms in Molecules: A Quantum Theory* (Oxford University Press, New York, 1990).
[20] G. Cinader, M. Peretz, D. Zamir, and Z. Hadari, Phys. Rev. B **8**, 4063 (1973).
[21] H. H. Hill, in *Plutonium and Other Actinides*, edited by W. N. Miner (AIME, New York, 1970), Vol. 17, p. 2.
[22] R. Troc and W. Suski, J. Alloys Compd. **219**, 1 (1995).
[23] Y. B. Barash, J. Barak, and M. H. Mintz, Phys. Rev. B **29**, 6096 (1984).